Attenuation limit of silica-based hollow-core fiber at mid-IR wavelengths

Fei Yu, Peng Song, Dakun Wu, et al.

View Online   Export Citation   CrossMark

ARTICLES YOU MAY BE INTERESTED IN

Fabrication and non-destructive characterization of tapered single-ring hollow-core photonic crystal fiber
APL Photonics 4, 056105 (2019); https://doi.org/10.1063/1.5093474

Electromechanical Brillouin scattering in integrated planar photonics
APL Photonics 4, 080802 (2019); https://doi.org/10.1063/1.5108672

Antiresonant reflecting optical waveguides in SiO_2-Si multilayer structures
Applied Physics Letters 49, 13 (1986); https://doi.org/10.1063/1.97085

Attenuation limit of silica-based hollow-core fiber at mid-IR wavelengths

View Online   Export Citation   CrossMark

Fei Yu,[1,2] ![ID] Peng Song,[1,3] Dakun Wu,[2,4] ![ID] Tim Birks,[1] David Bird,[1] and Jonathan Knight[1,a] ![ID]

AFFILIATIONS

[1] Centre for Photonics and Photonic Materials, Department of Physics, University of Bath, Claverton Down, Bath, BA2 7AY, United Kingdom

[2] Key Laboratory of Materials for High Power Laser, Shanghai Institute of Optics and Fine Mechanics, Chinese Academy of Sciences, Shanghai 201800, China

[3] School of Physics and Technology, University of Jinan, Jinan, Shandong, 250022, China

[4] Center of Materials Science and Optoelectronics Engineering, University of Chinese Academy of Sciences, Beijing 100049, China

[a] j.c.knight@bath.ac.uk

ABSTRACT

We study the mid-infrared attenuation of antiresonant hollow-core fiber made of fused silica glass. The role of absorptive losses increases with wavelength but can be minimized by reducing the overlap of the trapped light with the silica. We show that this overlap is least at the lowest-order antiresonance condition, corresponding to the thinnest core wall, and for higher resonances scales with the core wall thickness. A record-low minimum attenuation of 18 dB/km measured in our fiber at 3.1 μm wavelength is not limited by silica absorption. We measured 40 dB/km attenuation at 4 μm wavelength, where the attenuation of bulk silica is 860 dB/m. We show that this corresponds to a modal overlap of 2.81×10^{-5} which is in good agreement with simulations, suggesting that at this wavelength, attenuation is limited by silica absorption. This enables us to predict the achievable attenuation at longer wavelengths as well. Extrinsic losses due to gaseous molecular absorption may make demonstration of such losses difficult in some spectral bands. In contrast to shorter wavelengths, where leakage loss is the primary attenuation mechanism, introducing additional elements into the cladding design is unlikely to reduce the attenuation further, and further loss reduction would require a larger core size.

I. INTRODUCTION

Hollow-core (HC) waveguides were originally developed for electromagnetic wave transmission at long wavelengths from the microwave[1] to the far/mid-infrared[2] where material absorption is dominant. By using highly reflective material (metal or multilayer coating) and a large core design, improved transmission performance from several dB/m to 0.1 dB/m could be reached even in a simple tube waveguide, although only over short lengths due to fabrication issues.[2]

The invention of a photonic-bandgap hollow-core fiber (PBG-HCF)[3] greatly enlarged the available parameter space for hollow-core waveguide design. Thanks to the photonic bandgap effect arising from a periodic index variation in the cladding, the attenuation of hollow-core waveguides in the 1–2 μm spectral band was reduced to tens of decibels per kilometer and below in a small core of tens of micrometers, while the bend loss was no longer an issue.[4] For the first time, the use of hollow-core waveguides at near-infrared and visible wavelengths became an attractive proposition.[5–7] The lowest attenuation reported to date in a hollow-core waveguide was 1.2 dB/km at 1620 nm in a PBG-HCF[6] made of fused silica. High purity silica has been widely used as an optical fiber material for its high transparency in the visible and near-IR spectral range as well as its mechanical robustness, high chemical resistance, and good biomedical compatibility. The gentle slope of its thermal viscosity curve leaves a broad fabrication window for microstructured optical fibers. However, silica rapidly becomes opaque at 2.5 μm and longer wavelengths, with the phonon absorption rising from tens of

decibels per meter to tens of thousands. Nevertheless, the attenuation of PBG-PCF in the mid-infrared has been shown to be around 1% of the bulk material absorption,[8,9] which is only possible because of the low overlap of the guided light with the glass. Further significant reduction of this overlap below 1% was found to be challenging due to a range of design and fabrication issues.[6,8]

Since 2011, a new family of fiber designs has emerged. Antiresonant hollow-core fibers (AR-HCFs) are based on an antiresonant core wall and a simple cladding structure.[10–12] Unlike the PBG-HCF, the AR-HCF does not require a regular 2-dimensional array of identical air holes to confine the light to the core. A thin glass membrane can reflect the light effectively at glancing incidence under antiresonant conditions as in a Fabry–Pérot resonator.[13] The use of a negative curvature for the core wall shape[14] and control of the size of the ring of air holes immediately outside the core wall enables the leakage loss of AR-HCF to be further reduced. AR-HCFs based on these design concepts have demonstrated below 2 dB/km attenuation at around 1550 nm,[15,16] almost outperforming PBG-HCF. Theoretical studies suggest that AR-HCF may eventually demonstrate lower attenuation than the current state-of-the-art standard optical fiber, where losses are limited by Rayleigh scattering and by absorption.[17,18]

The simplicity of AR-HCF makes it possible to scale the fiber dimensions for different transmission windows from the UV,[19,20] through visible[21] and near-infrared[15] to the mid-infrared.[10,22] At mid-infrared wavelengths, 30 dB/km loss[22] and less[23] have been reported in silica-based AR-HCF around 3 μm wavelength and 100 dB/km at 4 μm.[24] By using chalcogenide glass instead of fused silica, a transmission window has been demonstrated at longer wavelengths with approximately 5 dB/m attenuation at 10 μm wavelength.[25] Despite a low material absorption, relatively high loss has been found in a chalcogenide-based hollow-core fiber due to increased leakage losses arising as a consequence of the challenges of fiber fabrication. The low-loss performance of AR-HCF at long wavelengths enables high-power mid-infrared laser beam delivery.[26] By filling an AR-HCF with molecular gases, novel light sources have been demonstrated at mid-IR wavelengths based on optically pumped gas lasing and stimulated Raman scattering.[23,27–30] These systems offer the merits of fiber lasers such as excellent laser beam quality, high power conversion efficiency, stability, and compactness.

In this paper, we focus on the limits to the attainable attenuation of AR-HCF at mid-infrared wavelengths. Our simulations show that using current designs, the material absorption of the silica glass plays a limiting role in the attainable attenuation of AR-HCF at 4 μm wavelength and beyond. We demonstrate an attenuation of 40 dB/km at 4 μm wavelength where the material absorption of bulk fused silica is 860 dB/m.

II. LOSS MECHANISMS OF AR-HCF IN THE MID-IR SPECTRAL BAND

There are a range of loss mechanisms which contribute to the overall attenuation in AR-HCF, and their relative significance depends strongly on wavelength. In the mid-IR spectral band, the most significant are leakage loss, material absorption by the bulk silica, and molecular absorption by gaseous species in the fiber core. Surface scattering loss,[5] which dominates the attenuation of

PBG-HCF at shorter wavelengths and may be a concern for AR-HCF in that spectral band as well, is of little consequence in the mid-IR due to the relatively low field strengths at the glass-air interfaces in AR-HCF, the scaling of scattering with wavelength, and the dominance of other loss mechanisms.

A. Leakage loss

Modes of AR-HCF are leaky in nature, and the light guidance can be broadly described by the ARROW model.[13] At wavelengths corresponding to resonances of the core wall, the optical power transits the core wall and is lost through scattering, leakage, or absorption.[13] The resonance wavelengths therefore define the edges of the fiber's transmission bands, approximated by

$$\lambda_m = \frac{2n_1 d}{m} \sqrt{\left(\frac{n_2}{n_1}\right)^2 - 1}, \tag{1}$$

where n_1 is the refractive index of the core and n_2 is the fiber material, d is the thickness of the core wall, and m is an integer, standing for the order of resonance.

At antiresonant wavelengths, the interference between the reflections from the glass-air interfaces can theoretically reduce the leakage losses to less than 0.1 dB/km,[17] making AR-HCF a candidate to break the current loss floor of a conventional single-mode silica fiber. Additional constructive reflections from interfaces have been theoretically demonstrated key to reaching this goal. In 2017, Bird analytically modeled the simplest AR-HCF consisting of concentric glass and air layers and derived the leakage loss formula,[18]

$$\alpha_{CL} = 8.686 \left(\frac{x_0}{2\pi}\right)^{N+2} \frac{1}{2} \frac{n^{2(N+1)} + 1}{(n^2 - 1)^{(N+1)/2}} \frac{\lambda^{N+2}}{r_c^{N+3}} \prod_{i=1}^{N} \frac{1}{\sin^2 \phi_i} \quad (\text{in dB/m}), \tag{2}$$

where α_{CL} is the leakage loss of HE/EH modes in the antiresonant hollow-core fibers, N is the number of glass and air antiresonant layers, x_0 is the mth zero of Bessel function J_{n-1} for HE_{nm} modes or of J_{n+1} for EH_{nm} modes, n is the refractive index of glass, λ is the wavelength, r_c is the core radius, and ϕ_i are phase angles corresponding to each successive layer.

Equation (2) explicitly shows that the leakage loss is closely related with the number of layers N in the radial direction and the phase lags ϕ_i of each layer. In practice, enlarging the core size r_c is the most effective means to reduce the leakage loss of AR-HCF.

B. Material loss

Absorption by the solid material used to define the structure contributes significantly to the overall fiber loss because although the overlap between this material and modal field of interest is low, the material absorption becomes very high in the mid-infrared. The absorption of fused silica rises by over four orders of magnitude from 2.5 μm to 5 μm wavelength. The modal overlap can be defined as

$$\eta = \frac{\iint_{S_2} \left|\overrightarrow{P}_z\right| dx dy}{\iint_{S_1} \left|\overrightarrow{P}_z\right| dx dy}, \tag{3}$$

where $\overrightarrow{P}_z$ is the Poynting vector along the light propagation direction z in the fiber, S_1 is the whole cross section of the fiber, and S_2 is the region of the solid material.

To link with the experiment, the modal overlap factor can also be calculated using

$$\eta = \frac{\alpha_{total} - \alpha_{CL}}{\alpha_{abs}}, \qquad (4)$$

where α_{total} is the overall loss that can be reliably compared to the experiment and α_{CL} is the leakage loss from the numerical simulation. α_{abs} is the bulk absorption of the fiber material determined by measurement.

A larger core helps reduce η and consequently the attenuation due to material absorption. The best overlap η achieved in PBG-HCF was demonstrated to be 0.5%[6] and 0.1% according to the simulation.[8] In AR-HCF, an enlarged core size[11,12] easily allows η to be reduced to 10^{-4}[24] or even less. This very small mode overlap makes AR-HCF attractive for light transmission at wavelengths where material absorption is strong, i.e., deep UV and mid-infrared, or where overlap with the glass is undesirable for other reasons.

C. Molecular gases in the fiber core

The mid-infrared is often referred to as the "spectral fingerprint" region because so many molecular species exhibit fundamental absorption resonances at these wavelengths. This includes species that are highly abundant in the atmosphere (H_2O and CO_2) as well as more exotic species that have been identified inside fabricated fibers but are not so apparent in the atmosphere. Within the spectral range under investigation in this work,[31] the atmosphere exhibits a strong band of absorption lines due to CO_2 and H_2O centered around 2.8 μm wavelength, a weaker series of absorption lines due to H_2O up to around 3.5 μm, a transmission window between 3.5 μm and perhaps 4.1 μm, and then a strong CO_2 absorption band at around 4.2 μm. In fabricated fibers, we also identify a rovibrational absorption band between 3.2 and 3.8 μm that we attribute to the presence of HCl in the fiber core.[22] This is likely to be a remnant of the halogenated precursors used in the fabrication of synthetic silica glass.

During fabrication, our fibers are filled with nitrogen, but the ends are not sealed and are exposed to the atmosphere in the laboratory. It is therefore inevitable that there is gradual ingress of atmospheric gases (driven in part by thermal fluctuations in the laboratory) into the fiber core. The HCl is presumably present throughout the fiber length, although our experience is that it can be removed by careful purging.

III. EFFECT OF VARYING THE CORE WALL THICKNESS

We use an ideal design of AR-HCF as shown in Fig. 1 (*left*) and numerically study the dependence of loss on the fiber structure. In Fig. 1 (*left*), the capillary tubes forming the cladding are identical, with an inner radius r_t of 27 μm. The fiber core radius r_c is fixed at 54 μm which is defined by a circle inscribed with all capillaries in the cladding. The chosen geometric parameters of AR-HCF are achievable in the practical fabrication for light transmission at mid-infrared wavelengths.

Using the finite-element method software COMSOL, we simulate the leakage and material losses of the fundamental mode in AR-HCF at 4 μm wavelength when varying the cladding capillary thickness d, i.e., the core wall thickness. We assume at 4 μm the silica refractive index is 1.389[32] and the bulk absorption is 860 dB/m.[33] It is noted that the gap between capillaries in the cladding slightly changes with d and this minor difference can be neglected because the size of gap is large compared to d.

In Fig. 1 (*right*), as the core wall thickness is scanned from 0.2 μm to 4.5 μm, both the leakage and material losses reflect the resonances and antiresonances of the cladding capillaries predicted by Eq. (1). Two polarizations are identified in the simulation presenting almost identical loss properties, and the average of losses and modal overlap are shown in Fig. 1 (*right*). As shown, for a certain capillary gap and resonance of air regions, the leakage loss (blue dot curves, left hand axis) is determined by the phase lag in the core wall only (while r_t is fixed) rather than the absolute core wall thickness, which agrees with the prediction of Eq. (2). The minimum leakage loss is very similar for both the lowest antiresonance [*circa* 1.2 μm core wall thickness, with $m = 0.5$ in Eq. (1)] and the next antiresonance condition [*circa* 3.2 μm with $m = 1.5$ in Eq. (1)]. However, the material losses (blue circle curves, left axis) and the modal overlap (two red curves on the right axis) change with both the phase condition and the core wall thickness. A thinner core wall thickness for the same phase lag is demonstrated to reduce the modal overlap. Around the lowest antiresonance, the modal overlap ratio defined by Eqs. (3) and (4) is 2.55×10^{-5} and 3.26×10^{-5}, respectively. For the higher antiresonance, the modal overlap increases to 7.19×10^{-5} and 9.85×10^{-5}. The higher antiresonance condition leads to absorptive and overall losses that are roughly three times higher than those found for the lowest antiresonance, as a consequence of the correspondingly thicker core walls, as might be naively expected. In the current design of AR-HCF, 28.1 dB/km at 4 μm wavelength is numerically
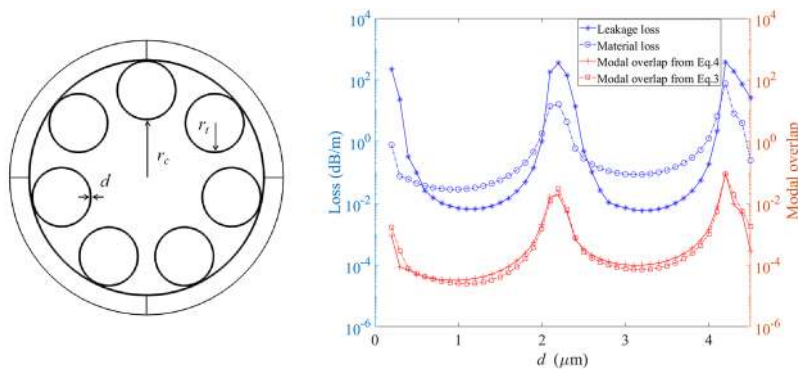
FIG. 1. *Left*: AR-HCF model used in simulations. *Right*: simulated leakage and material losses of the fundamental mode (blue, left axis) and modal overlap ratio (red, right axis) at 4 μm wavelength as a function of core wall thicknesses. All curves are the average of two polarization modes.
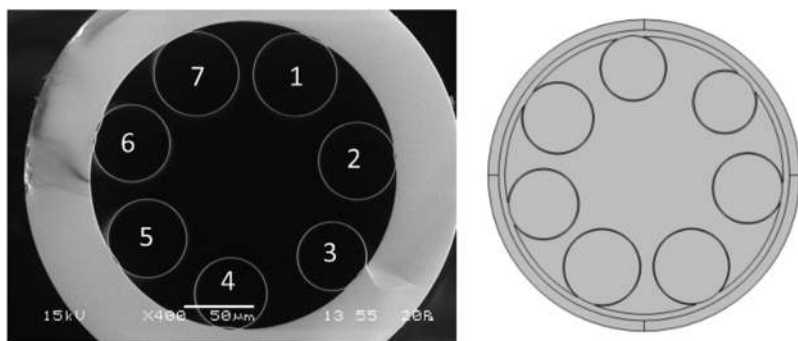
FIG. 2. *Left*: SEM picture of the fabricated AR-HCF made of F300 fused silica glass. The average core diameter is about 105 μm defined by the inscribed circle of capillaries in the cladding. The details of fiber geometry can be found in Table I. *Right*: model used in the FEM numerical simulation of the AR-HCF on the left. Details can be found in Ref. 34.

predicted as the minimum material loss using silica, and the lowest overall loss 35.1 dB/km is found for the lowest-order antiresonance condition.

It should also be noted that practical interest has usually been in the low-loss spectral regions, where the core wall is close to antiresonance. Although we do not doubt the accuracy of our numerical simulations in the antiresonance regions, the computed attenuation around the resonances can be expected to depend strongly on the definition of the fiber structure further away from the hollow core, and so our simulations may not reflect experimental realizations in this high-loss regime.

IV. EXPERIMENTS

In this section, we demonstrate the attenuation limits of the AR-HCF fabricated using silica glass.

Figure 2 (*left*) is the scanning electron microscope picture of an AR-HCF made of Heraeus F300 fused silica glass. A length of 226 m of AR-HCF was fabricated using the stack-and-draw method. The capillaries in the cladding were kept from collapsing by pressurization during fiber fabrication. Technical challenges during fabrication limited the uniformity of the fiber cross section. Longitudinal uniformity was checked by comparing the two fiber ends, which had core diameters of 110 μm–105 μm, respectively. Low drawing temperature and a draw-down-ratio (preform to fiber) of approximately 30 were used to minimize the nonuniformity of fiber structure along the length. In Fig. 2 (*left*), the maximum thickness of the core wall is 990 nm, which gives the first resonance wavelength to be around 2.04 μm using a refractive index of 1.4373[33] according to Eq. (1). Table I summarizes the wall thickness of all 7 capillaries. Details of the COMSOL model in Fig. 2 (*right*) can be found in Ref. 34.
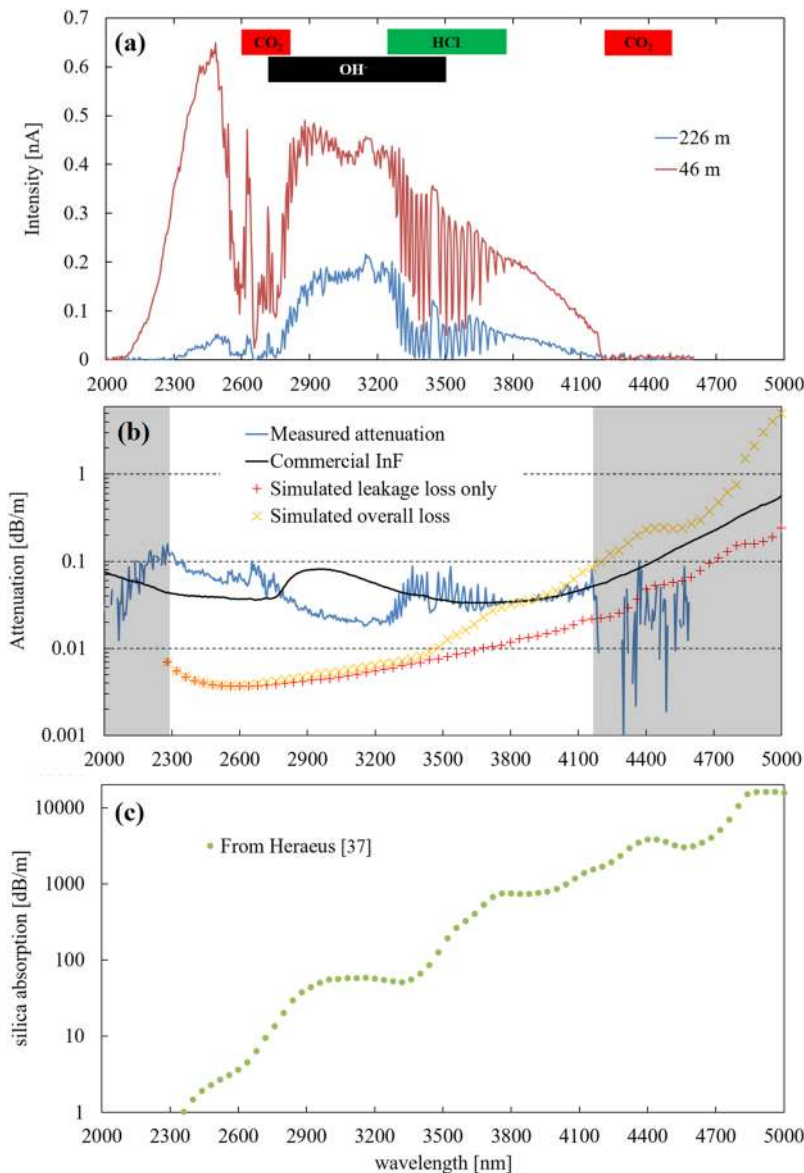
Measured fiber transmission spectra in a cutback measurement from 226 m to 46 m are shown in Fig. 3(a). To avoid any concerns

about bend loss, the fiber was rewound in loose loops with about 1 m diameter. A stabilized tungsten lamp was used as the white light source which maintains a constant emission spectrum for hours. To avoid the possible influence of variable insertion loss during the cutback measurement, the transmission spectra in Fig. 3(a) are average of multiple measured transmission spectra for the same fiber lengths. In each transmission measurement, the fiber end was recleaved and plugged in the monochromator using a bare fiber adaptor. Measurements of both short and long fibers were repeated at two different spectral resolutions, giving results in good agreement and adding further confidence to our technique. Due to the decreasing efficiency of the tungsten lamp and the reduced response of the indium antimonide detector at long wavelengths in the monochromator, no transmitted light could be detected beyond the strong absorption lines at 4.2 μm wavelength. Single-mode transmission can be expected in both fiber lengths because of efficient higher-order mode filtering due to core-cladding mode coupling in the current fiber design.[35]

The blue line in Fig. 3(b) is the fiber attenuation from the cutback measurement. A minimum of 18 dB/km is measured at 3160 nm wavelength and 40 dB/km at 4 μm. The measured fiber attenuation is comparable to that of a commercially available multimode InF$_3$ fiber,[36] shown as the black line in Fig. 3(b), although significantly lower in the spectral range 2.9–3.2 μm. (The attenuation of the InF$_3$ fiber was measured[36] in a fiber with a 100 μm core and 0.26 NA.) The absorption spectrum of silica in Fig. 3(c) is based on information provided by Heraeus and available in Ref. 37. The simulation in Fig. 3(b) shows that, in the mid-infrared spectral range, the contribution from absorptive material loss to the total loss becomes comparable to leakage loss at wavelengths starting from 3 μm, as the material absorption exceeds 50 dB/m. The material loss becomes the dominant loss mechanism when the material absorption exceeds 600 dB/m around 3.7 μm. At 3.7 μm wavelength and beyond, the numerical simulation matches well with the experimentally measured fiber loss, corresponding to a calculated 2.81×10^{-5} modal field overlap with the silica glass in the cladding at 4 μm by Eq. (4) [3.07×10^{-5} modal field overlap by Eq. (3)]. At 4.96 μm, the simulation predicts 4.02 dB/m overall loss, while the fluoride fiber exhibits only about 0.5 dB/m. By linearly scaling up the fiber model [Fig. 2 (*right*)] by 1.25, the total loss at 5 μm wavelength is reduced to 0.69 dB/m, giving rise to 4.0×10^{-5} and 4.3×10^{-5} modal field overlap by Eqs. (3) and (4), respectively. Higher loss of the AR-HCF due to the silica absorption can be expected at even longer

TABLE I. Measured thicknesses of silica cladding capillaries.

Capillary#	1	2	3	4	5	6	7
Inner diameter $2r_t$ (μm)	58.7	54.3	48.4	50.7	55.4	54.3	59.5
Thickness d (nm)	630	760	990	790	770	910	710

FIG. 3. (a) Measured transmission spectra through 226 m and 46 m of the AR-HCF in the cutback measurement. Some gaseous molecular absorption features are identified. (b) Resulting fiber attenuation (blue line). The minimum attenuation is 18 dB/km at 3160 nm wavelength and 40 dB/km at 4 μm wavelength. The results in the gray region are dominated by noise. The commercial InF3 multimode fiber loss is plotted in black.[36] The simulated total loss (including material absorption) and the leakage loss of the AR-HCF are also plotted. (c) The material absorption of fused silica used in the simulation, available from Ref. 37.

wavelengths, which makes the light transmission in this spectral region using current AR-HCF designs uncompetitive with alternative technologies.

The minimum experimental loss is 18 dB/km around 3.2 μm wavelength, which is greater than the simulated value of 6.4 dB/km at that wavelength. The simulated minimum loss is only 3.7 dB/km at 2.6 μm, where the measurement is up to 60 dB/km. However, 2.6 μm corresponds to a region of strong molecular absorption lines, the presence of which is very clear from the cutback data [Fig. 3(a)]. The degraded experimental attenuation can likewise be attributed to the presence of gaseous molecular absorption lines in the spectral range to 3.5 μm[22] as well as the effect of variations of fiber geometry along the fiber length.

V. CONCLUSIONS

This paper reports on the design and demonstration of a silica-based AR-HCF for the mid-IR spectra region. We have demonstrated by numerical simulations that the lowest overlap between the confined mode and the silica glass is obtained when the core wall is at the lowest-order (thinnest) antiresonance condition. We predict that this overlap will be around 2.55×10^{-5} in an ideal AR-HCF and confirmed as 2.81×10^{-5} by analyzing the measured fiber loss at 4 μm wavelength. On the basis of existing data on the absorption of fused silica, we anticipate that this will result in an attenuation of 45 dB/km at 4 μm wavelength, which is in excellent agreement with the value of 40 dB/km measured in a fabricated fiber. A very similar

overlap can be expected for the same fiber design scaled to longer wavelengths, so we can predict that the attenuation of similar fibers at 5 μm wavelength would be around 0.69 dB/m. At shorter wavelengths (below 3.5 μm), absorptive losses are not the limiting factor in current fibers. Instead, a combination of extrinsic gaseous molecular absorption and structural variations along the fiber length leads to the predicted attenuation not being reached. Further reductions in attenuation beyond those predicted numerically in this work could be achieved by use of a larger core diameter (although being aware of the consequences for bending loss) or by fabricating fibers using different glasses with lower spectral absorption. Unlike at shorter wavelengths where leakage loss is an issue,[12,18,24] the use of additional antiresonant features in the cladding is not likely to reduce the attenuation. All data underlying the results presented in this paper can be found in Ref. 34.

ACKNOWLEDGMENTS

REFERENCES

[1] R. E. Collin, *Foundations for Microwave Engineering*, 2nd ed. (IEEE Press, 2001).

[2] J. A. Harrington, "A review of IR transmitting, hollow waveguides," Fiber Integr. Opt. **19**, 211–227 (2000).

[3] R. F. Cregan, B. J. Mangan, J. C. Knight, T. A. Birks, P. J. St. Russell, P. J. Roberts, and D. C. Allan, "Single-mode photonic band gap guidance of light in air," Science **285**, 1537–1539 (1999).

[4] P. S. J. Russell, "Photonic-crystal fibers," J. Lightwave Technol. **24**, 4729–4749 (2006).

[5] P. J. Mosley, W. C. Huang, M. G. Welch, B. J. Mangan, W. J. Wadsworth, and J. C. Knight, "Ultrashort pulse compression and delivery in a hollow-core photonic crystal fiber at 540 nm wavelength," Opt. Lett. **35**, 3589–3591 (2010).

[6] P. J. Roberts, F. Couny, H. Sabert, B. J. Mangan, D. P. Williams, L. Farr, M. W. Mason, A. Tomlinson, T. A. Birks, J. C. Knight, and P. St. J. Russell, "Ultimate low loss of hollow-core photonic crystal fibres," Opt. Express **13**, 236–244 (2005).

[7] G. Bouwmans, F. Luan, J. Knight, P. St. J. Russell, L. Farr, B. Mangan, and H. Sabert, "Properties of a hollow-core photonic bandgap fiber at 850 nm wavelength," Opt. Express **11**, 1613 (2003).

[8] N. V. Wheeler, A. M. Heidt, N. K. Baddela, E. N. Fokoua, J. R. Hayes, S. R. Sandoghchi, F. Poletti, M. N. Petrovich, and D. J. Richardson, "Low-loss and low-bend-sensitivity mid-infrared guidance in a hollow-core-photonic-bandgap fiber," Opt. Lett. **39**, 295–298 (2014).

[9] J. D. Shephard, W. N. MacPherson, R. R. J. Maier, J. D. C. Jones, D. P. Hand, M. Mohebbi, A. K. George, P. J. Roberts, and J. C. Knight, "Single-mode mid-IR guidance in a hollow-core photonic crystal fiber," Opt. Express **13**, 7139 (2005).

[10] A. D. Pryamikov, A. S. Biriukov, A. F. Kosolapov, V. G. Plotnichenko, S. L. Semjonov, and E. M. Dianov, "Demonstration of a waveguide regime for a silica hollow-core microstructured optical fiber with a negative curvature of the core boundary in the spectral region >3.5 μm," Opt. Express **19**, 1441–1448 (2011).

[11] C. Wei, R. J. Weiblen, C. R. Menyuk, and J. Hu, "Negative curvature fibers," Adv. Opt. Photonics **9**, 504–561 (2017).

[12] F. Yu and J. C. Knight, "Negative curvature hollow-core optical fiber," IEEE J. Sel. Top. Quantum Electron. **22**, 146–155 (2016).

[13] N. M. Litchinitser, A. K. Abeeluck, C. Headley, and B. J. Eggleton, "Antiresonant reflecting photonic crystal optical waveguides," Opt. Lett. **27**, 1592–1594 (2002).

[14] Y. Y. Wang, N. V. Wheeler, F. Couny, P. J. Roberts, and F. Benabid, "Low loss broadband transmission in hypocycloid-core Kagome hollow-core photonic crystal fiber," Opt. Lett. **36**, 669–671 (2011).

[15] S.-F. Gao, Y.-Y. Wang, W. Ding, D.-l. Jiang, S. Gu, X. Zhang, and P. Wang, "Hollow-core conjoined-tube negative-curvature fibre with ultralow loss," Nat. Commun. **9**, 2828 (2018).

[16] "Record low-loss 1.3 dB/km data transmitting antiresonant hollow core fibre," in *2018 European Conference on Optical Communication (ECOC)*, edited by T. D. Bradley, J. R. Hayes, Y. Chen, G. T. Jasion, S. R. Sandoghchi, R. Slavik, E. N. Fokoua, S. Bawn, H. Sakr, I. A. Davidson, A. Taranta, J. P. Thomas, M. N. Petrovich, D. J. Richardson, and F. Poletti (IEEE, 2018).

[17] F. Poletti, "Nested antiresonant nodeless hollow core fiber," Opt. Express **22**, 23807–23828 (2014).

[18] D. Bird, "Attenuation of model hollow-core, anti-resonant fibres," Opt. Express **25**, 23215–23237 (2017).

[19] S.-F. Gao, Y.-Y. Wang, W. Ding, and P. Wang, "Hollow-core negative-curvature fiber for UV guidance," Opt. Lett. **43**, 1347–1350 (2018).

[20] F. Yu, M. Cann, A. Brunton, W. Wadsworth, and J. Knight, "Single-mode solarization-free hollow-core fiber for ultraviolet pulse delivery," Opt. Express **26**, 10879–10887 (2018).

[21] S.-F. Gao, Y.-Y. Wang, X.-L. Liu, C. Hong, S. Gu, and P. Wang, "Nodeless hollow-core fiber for the visible spectral range," Opt. Lett. **42**, 61–64 (2017).

[22] F. Yu, W. J. Wadsworth, and J. C. Knight, "Low loss silica hollow core fibers for 3-4 μm spectral region," Opt. Express **20**, 11153–11158 (2012).

[23] M. R. Abu Hassan, F. Yu, W. J. Wadsworth, and J. C. Knight, "Cavity-based mid-IR fiber gas laser pumped by a diode laser," Optica **3**, 218 (2016).

[24] F. Yu and J. C. Knight, "Spectral attenuation limits of silica hollow core negative curvature fiber," Opt. Express **21**, 21466–21471 (2013).

[25] V. S. Shiryaev, "Chalcogenide glass hollow-core microstructured optical fibers," Front. Mater. **2**, 3439 (2015).

[26] A. Urich, R. R. J. Maier, F. Yu, J. C. Knight, D. P. Hand, and J. D. Shephard, "Flexible delivery of Er:YAG radiation at 2.94 μm with negative curvature silica glass fibers: A new solution for minimally invasive surgical procedures," Biomed. Opt. Express **4**, 193–205 (2013).

[27] M. Xu, F. Yu, and J. Knight, "Mid-infrared 1 W hollow-core fiber gas laser source," Opt. Lett. **42**, 4055–4058 (2017).

[28] F. B. A. Aghbolagh, V. Nampoothiri, B. Debord, F. Gerome, L. Vincetti, F. Benabid, and W. Rudolph, "Mid IR hollow core fiber gas laser emitting at 4.6 μm," Opt. Lett. **44**, 383 (2019).

[29] A. V. Gladyshev, A. F. Kosolapov, M. M. Khudyakov, Y. P. Yatsenko, A. N. Kolyadin, A. A. Krylov, A. D. Pryamikov, A. S. Biriukov, M. E. Likhachev, I. A. Bufetov, and E. M. Dianov, "4.4-μm Raman laser based on hollow-core silica fibre," Quantum Electron. **47**, 491–494 (2017).

[30] "Raman generation in 2.9–3.5 μm spectral range in revolver hollow-core silica fiber filled by H$_2$/D$_2$ mixture," in *Proceedings of the Conference on Lasers and Electro-Optics, STU1K*, edited by A. V. Gladyshev, A. F. Kosolapov, M. M. Khudyakov, Y. P. Yatsenko, A. K. Senatorov, A. N. Kolyadin, A. A. Krylov, V. G. Plotnichenko, M. E. Likhachev, I. A. Bufetov, and E. M. Dianov (Optical Society of America, 2017).

[31] H. Horvath, "Atmospheric light absorption—A review," Atmos. Environ., Part A **27**, 293–317 (1993).

[32] C. Z. Tan, "Determination of refractive index of silica glass for infrared wavelengths by IR spectroscopy," J. Non-Cryst. Solids **223**, 158–163 (1998).

[33] R. Kitamura, L. Pilon, and M. Jonasz, "Optical constants of silica glass from extreme ultraviolet to far infrared at near room temperature," Appl. Opt. **46**, 8118–8133 (2007).

[34] See https://doi.org/10.15125/BATH-00671 for all data underlying the results in this paper.

[35] F. Yu, M. Xu, and J. C. Knight, "Experimental study of low-loss single-mode performance in anti-resonant hollow-core fibers," Opt. Express **24**, 12969–12975 (2016).

[36] See https://www.thorlabs.de/newgrouppage9.cfm?objectgroup_id=7062#ad-image-0 for attenuations of commercial InF$_3$ fiber.

[37] See https://www.heraeus.com/en/hqs/fused_silica_quartz_knowledge_base/t_calc/transmission_calculator.aspx?selection=suprasil_3001_3002_300&chart=0&rangeX=120,5000&rangeY=0,100 for the measured transmission of F300 fused silica for different thicknesses.